

de Sénarmont Bias Retardation in DIC Microscopy

Stanley Schwartz¹, Douglas B. Murphy²,
Kenneth R. Spring³, and Michael W. Davidson⁴

¹Bioscience Department, Nikon Instruments, Inc., 1300 Walt Whitman Road, Melville, New York 11747.

²Department of Cell Biology and Anatomy and Microscope Facility, Johns Hopkins University School of Medicine, 725 N. Wolfe Street, 107 WBSB, Baltimore, Maryland 21205.

³National Heart, Lung, and Blood Institute, National Institutes of Health, Building 10, Room 6N260, Bethesda, Maryland 20892

⁴National High Magnetic Field Laboratory, Florida State University, Tallahassee, Florida 3231

Keywords: microscopy, de Sénarmont, Henri Hureau de Sénarmont, Francis Smith, Georges Nomarski, William Hyde Wollaston, Michel-Levy color chart, contrast-enhancement techniques, depth of field, bias, retardation, compensating, plates, DIC, differential interference, contrast, prisms, compensators, shadow-cast, relief, pseudo, three-dimensional, birefringence, optical staining, sectioning, spherical aberrations, wavefronts, shear, fast, slow, axes, axis, linear, circularly, elliptically, polarized light, polarizers, analyzers, orthogonal, path, differences, OPD, gradients, phase, ordinary, extraordinary, maximum extinction, quarter-wavelength, full-wave plates, first-order red, halo, artifacts, interference plane, VEC, video enhanced, VE-DIC, Newtonian, interference colors, Nikon, Eclipse E600, microscopes, buccal, mucosa, epithelial, cheek cells, ctenoid, fish scales, Obelia, hydroids, polyps, coelenterates, murine, rodents, rats, mice, mouse, kidneys, Volvox, colony, mucilage, gonidia, green algae, cilia, nucleus, cellular membranes, high refractive index boundaries, cellular biology, microtubules, bacteria, flagella, miniature organelles, ergonomics

Introduction

Living cells and other transparent, unstained specimens are often difficult to observe under traditional brightfield illumination using the full aperture and resolution of the microscope objective and condenser system (1, 2). Phase contrast, first developed by Frits Zernike in the 1930s, is often employed to image these challenging specimens, but the technique suffers from halo artifacts, is restricted to very thin specimen preparations, and cannot take advantage of the full condenser and objective apertures.

Differential interference contrast (DIC) microscopy was first suggested and devised by Francis Smith in 1955, who built a modified polarized light microscope having Wollaston prisms added to the front focal plane of the condenser and the rear focal plane of the objective. Because of their design limitations, Wollaston prisms were subsequently replaced with a more advanced system, introduced by French scientist Georges Nomarski, which enabled the prisms to be physically located some distance away from the condenser and objective aperture conjugate planes. This modification allows the use of standard microscope optical components in modern DIC systems, and is currently enjoying widespread application (3-5).

In a manner similar to phase contrast, DIC microscopy is useful for visualizing transparent specimens, but DIC does not suffer from the halo artifacts and masked apertures inherent with phase contrast optics, and has the ability to produce excellent images with relatively thick specimens. In addition, DIC images can be easily manipulated using digital and video imaging techniques to further enhance contrast.

The differential interference contrast effect functions by converting gradients in specimen optical path length into amplitude (intensity, as illustrated in Figure 1) differences that can be visualized as improved contrast in the microscope eyepieces (or recorded on film or digitally). The primary determining factors in specimen optical path

length are the refractive index difference between the specimen and its surrounding medium, and the geometrical distance traversed by the sheared wavefronts between two points on the optical path. Images produced by DIC optical systems have a distinctive shadow-cast appearance and appear to be pseudo three-dimensional, as if they were illuminated from a highly oblique light source originating from a single azimuth (1). In general, DIC is useful for determining the orientation of phase gradients and for utilizing the full objective aperture to produce thin optical sections of specimens that are devoid of obscuring disturbances positioned beyond the immediate focal plane.

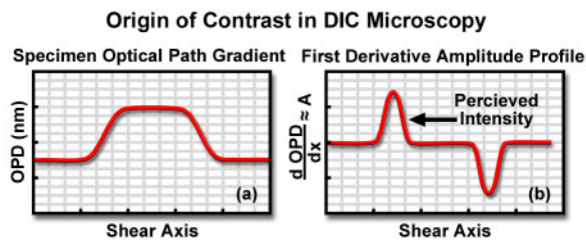


Figure 1. Differential interference contrast functions by converting gradients in specimen optical path length into amplitude differences that can be visualized as improved contrast in the microscope eyepieces. The graphs illustrate (a) theoretical specimen optical path gradient in the direction of the prism shear axis, and (b) the first derivative amplitude profile of the OPD.

In traditional differential interference contrast microscope system designs, bias retardation is introduced into the optical train by translating one of the matched (condenser and objective) Nomarski or modified Wollaston prisms across the optical axis of the microscope to produce a constant optical path difference (as discussed below). The same effect can also be achieved through the application of a fixed Nomarski prism system and a simple

de Sénarmont compensator consisting of a quarter-wavelength retardation plate in conjunction with either the polarizer or analyzer (2).

The basic de Sénarmont configuration consists of a rotatable polarizer (or analyzer) and a quarter-wavelength retardation plate, which are combined into a housing that is secured with a setscrew onto the main light port in the base of the microscope. The retardation plate is held in a preset orientation, while the polarizer is rotated through 90 degrees (plus or minus 45 degrees) around the optical axis of the microscope. Depending upon the orientation of the polarizer with respect to the retardation plate, the de Sénarmont compensator will illuminate the microscope optical train with linear, elliptical, or circularly polarized light.

Polarized wavefronts exiting the de Sénarmont compensator first encounter the fixed Nomarski prism in the microscope condenser, and are subsequently re-oriented and sheared to produce orthogonal components (an **ordinary** and an **extraordinary** wavefront) having vibration directions at a 45-degree angle to the plane of polarized light emerging from the de Sénarmont compensator. The condenser lens system focuses the sheared wavefronts into parallel components and projects them onto the specimen. Light leaving the specimen is collected by the objective and focused onto the interference plane of the second fixed Nomarski prism located in a frame housed in the microscope nosepiece. The objective Nomarski prism, which is matched to the condenser prism and inverted, recombines the sheared wavefronts into coaxial orthogonal components. Although linearly polarized light exiting the objective Nomarski prism is blocked by the analyzer, elliptically and circularly polarized light components are partially transmitted, forming an image of the specimen.

Wollaston and Nomarski Prisms

The critical elements in differential interference contrast microscopy are matched birefringent Wollaston and/or Nomarski prisms, which are inserted into the microscope optical pathway with their shear axes oriented at a 45-degree angle (northwest to southeast) to the polarizer and analyzer (5). Wollaston prisms are constructed of two precisely ground and polished wedge-shaped slabs of quartz having perpendicular orientations of the optical axis and cemented together at the hypotenuse to generate an optically anisotropic compound plate. Incident linearly polarized wavefronts entering a Wollaston prism (oriented at a 45-degree angle to the prism optical axes) are divided into two separate orthogonal waves, termed the ordinary and the extraordinary wave.

Because they are derived from localized areas on a single source (generally, the filament of a tungsten-halogen lamp), the orthogonal wavefronts generated by a Wollaston prism are coherent, have identical amplitudes, and propagate in the same direction through the lower prism wedge (see Figure 2(a)). The ordinary wave travels through the prism in a direction that is perpendicular to the optical axis, while the extraordinary wave is ori-

Wollaston and Nomarski Prisms for DIC Microscopy

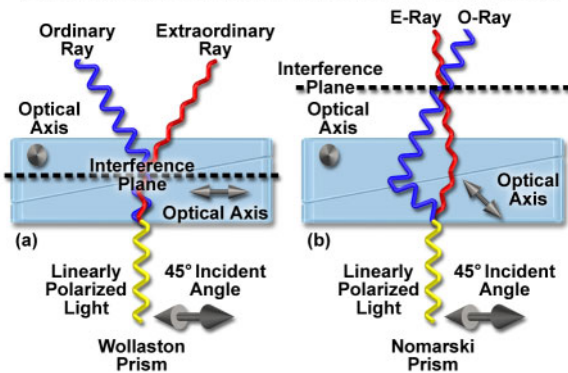


Figure 2. Wavefront shear by Wollaston (a) and Nomarski (b) prisms. Linearly polarized light enters the prisms from the lower section of the figure oriented at a 45-degree angle with respect to the optical axis of the lower wedge. The interference plane lies in the center of the Wollaston prism, but is positioned outside the Nomarski prism. The ordinary wavefront is shown in red while the extraordinary wavefront is blue.

ented parallel to the axis. In addition, varying dielectric properties along these perpendicular axes result in one wave traveling through the prism at a higher velocity than the other. The ordinary wave proceeds through the prism along the faster axis of the wavefront ellipsoid (having a lower refractive index), and the extraordinary wave traverses the slower axis (higher refractive index).

At the refractive index junction between the cemented quartz wedges, an angular splitting or **shear** of the wavefronts occurs, resulting in the waves becoming spatially separated by an angle defined as the **shear angle**. In addition, the wavefronts exchange identities at the prism wedge boundary, with the ordinary wave becoming the extraordinary wave and vice versa. The shear angle and separation distance is constant for all incident wavefronts across the prism, regardless of the entry point, and the direction of wavefront shear is defined by the prism **shear axis**. This axis lies in the longitudinal plane of a Wollaston prism and is parallel to the direction of the optical axis of the lower quartz wedge. In general, the shear distance produced by a Wollaston (or Nomarski) prism is less than a micrometer so that no observable beam separation occurs in light emerging from the prism.

The refractive index difference experienced by the ordinary and extraordinary wavefronts results in varying propagation velocities for the two waves as they travel through the lower and upper sections of a Wollaston prism. In the lower half of the prism, the wavefronts undergo a phase shift that is exactly compensated in the upper half when the geometrical path through the lower and upper halves is identical. However, wavefronts traversing through points away from the center experience a longer journey through either the lower or upper half of the prism, which results in a constant phase shift per unit length in the direction of the shear axis. The phase shift is equal, but opposite, for the ordinary and extraordinary wavefronts. As a result, at one end of the prism, the ex-

traordinary wavefront emerges ahead of the ordinary wavefront, while at the corresponding position on the other end, the ordinary wavefront exits the prism before the extraordinary wavefront. The focal, or interference, plane of a Wollaston prism occurs in the center of the prism where the optical path between the lower and upper quartz wedges is equal. For this reason, it is often difficult (or impossible) to adapt a Wollaston prism for use with standard microscope objectives, which often have a rear focal plane (that must physically coincide with the Wollaston prism interference plane) buried deep inside a lens.

Similar to a conventional Wollaston prism, the basic Nomarski prism design (Figure 2(b)) also consists of two quartz wedges that are cemented together at the hypotenuse. The upper wedge is identical to a conventional Wollaston quartz wedge, but the lower wedge is modified by cutting the quartz crystal in a direction that yields an oblique optical axis with respect to the flat surface of the prism. When the wedges are combined to form a compound birefringent prism, the focal (interference) plane lies at a site several millimeters outside the prism plate. This effect occurs because shear takes place at the quartz-air interface in the lower prism wedge instead at the cemented boundary, as in a Wollaston prism. Refraction at the interface between the quartz wedges in a Nomarski prism causes the sheared wavefronts to converge with a crossover point outside the prism (as illustrated in Figure 2(b)). The actual position of the Nomarski prism focal plane can be adjusted over a range of several millimeters by altering the oblique angle of the optical axis in the lower quartz wedge utilized to construct the prism.

Modern DIC microscopes are usually constructed with Nomarski prisms to avoid the objective aperture clearance problem (1-4). In fact, the modified prisms are often employed for both beam shearing and recombination duty in the condenser and objective focal planes. Although there are fewer spatial constraints for condenser prisms, which can often be positioned precisely within the aperture plane, a Nomarski prism is still used in most cases. Nomarski prisms can be designed specifically for condensers to produce an interference plane that is located much closer to the prism than those constructed for use with objectives. As a result, aside from being mounted in frames having different geometries, the two Nomarski prisms found in modern DIC microscopes are often cut differently and are not interchangeable.

The de Sénarmont DIC Optical System

A traditional differential interference microscope optical system contains a polarizer located before the condenser and an analyzer (a second polarizer) inserted into the pathway above the objective, usually in an intermediate tube or combined in the frame with the objective Nomarski prism (2, 3, 6). The polarizer is oriented with the vibration plane transmission axis positioned East-West, while the analyzer is crossed with respect to the polarizer (transmission axis is North-South). Linear polarized light leaving the polarizer is separated into two components by a Nomarski prism housed in the condenser near the

conjugate focal plane of the iris diaphragm aperture. Incident wavefronts are sheared by the prism into orthogonal polarized components separated by less than a micrometer, rendered parallel by the condenser optical system, and then utilized to illuminate the specimen.

Positioned behind the objective in the optical pathway is a second Nomarski prism (usually housed in an adjustable sliding frame), which is utilized to recombine the sheared wavefronts in the conjugate plane of the rear aperture after they have been collected and focused by the objective. Components of circular and elliptically polarized light from the recombined wavefronts pass through the analyzer and subsequently undergo interference to generate the DIC image at the microscope intermediate image plane.

In a perfectly aligned DIC microscope, the condenser prism is imaged by the condenser and objective lens assemblies onto the objective prism so that wavefront shear between orthogonal wavefronts is matched at every point along the surface of the prisms, which are inverted with respect to one another. Translating either prism along the shear axis (perpendicular to the microscope optical axis) produces a wavefront mismatch that is uniform across the microscope aperture. Shifting the phase displacement of the ordinary wavefront with respect to the extraordinary wavefront through translation of a prism in the way just described is often termed **introduction of bias retardation** in DIC microscopy (1, 3). As one of the Nomarski prisms is shifted laterally (usually the objective prism), wavefront pairs contributing to the background become increasingly retarded and out of phase with one another. Thus, the polarization vector orientation of light emerging from the objective Nomarski prism can be adjusted from linear (no translation), through varying degrees of elliptical, and even to circular.

Introduction of bias retardation into a DIC optical system produces changes to the intensity (amplitude) levels of phase gradients in the specimen, which result in the generation of orientational-dependent bright highlights and dark shadows superimposed on a lighter background. Intensity gradients occur along the shear axis of the condenser and objective prisms, and generally appear to be originating from a 45-degree angle (northwest to southeast or vice versa) when the specimen is observed in the eyepieces. Shifting the prism in one direction or another across the microscope optical axis will vary the phase relationship between the orthogonal wavefronts, thus reversing the shadow-cast orientation in the specimen. The net result is to render the specimen image in pseudo three-dimensional relief where regions of increasing optical path length (sloping phase gradients) appear much brighter or darker, and those exhibiting decreasing path length appear in reverse.

An alternative technique for introduction of bias retardation, which is growing in popularity, is to mount a quarter-wavelength retardation plate in fixed orientation between the polarizer and condenser prism (termed **de Sénarmont** DIC compensation, as discussed above) and rotate either the polarizer or analyzer. At maximum extinction (matched prisms with no bias applied; see Figure

3(b)), the fast axis of the retardation plate is aligned with the transmission axis of the polarizer. Both optical units can be (and often are) contained within the same housing on the base of the microscope. An alternative location for the de Sénarmont compensator, in microscopes equipped with the appropriate intermediate tube, is between the objective prism and the analyzer.

In order to introduce bias using the de Sénarmont compensator, the polarizer transmission axis is rotated (up to plus or minus 45 degrees; see Figures 3(a) and 3(c)) with respect to the fast axis of the retardation plate, which remains fixed at a 90-degree angle relative to the analyzer transmission axis. When the compensator fast axis coincides (is parallel) with the transmission axis of the polarizer, only linearly polarized light passes through the de Sénarmont compensator to the condenser prism, as illustrated in Figure 3(b). However, when the polarizer transmission axis is rotated, wavefronts emerging from the quarter-wavelength retardation plate become elliptically polarized. Rotating the polarizer in one direction will produce right-handed elliptically polarized light (Figure 3(a)), while rotating the polarizer in the other direction will alter the vector trajectory to generate a left-handed elliptical sweep (illustrated in Figure 3(c)).

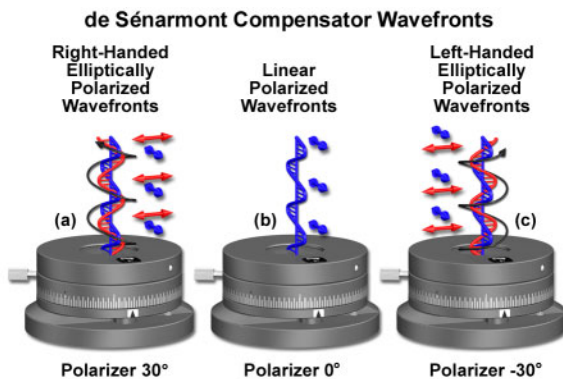


Figure 3. Wavefronts generated by a de Sénarmont compensator as a function of the polarizer rotation angle. (a) polarizer rotated 30 degrees from the quarter-wavelength retardation plate fast axis, (b) polarizer parallel to the retardation plate fast axis, and (c) polarizer rotated -30 degrees from the retardation plate fast axis.

When the orientation of the polarizer transmission axis reaches either plus or minus 45 degrees (equivalent to one-quarter wavelength of retardation), light passing through the compensator becomes circularly polarized (again in either a left-handed or right-handed sense). Because elliptically or circularly polarized light represents a phase difference between the ordinary and extraordinary wavefronts emerging from the de Sénarmont compensator, bias is introduced to the system when the wavefronts enter the condenser Nomarski beamsplitter prism and become sheared (Figure 4). Positive bias is obtained when the polarizer is rotated in one direction, while negative bias is introduced by rotating the polarizer in the opposite direction. The amount of relative re-

tardation introduced by a de Sénarmont compensator can be quantitatively determined according to the equation:

$$\text{Retardation (in nanometers)} = \theta\lambda / 180$$

where θ is the rotation angle (calculated in degrees) of the polarizer transmission axis in relation to the fast axis of the retardation plate, and λ is the average wavelength of light passing through the compensator. In the case of tungsten-halogen illumination, the wavelength is often taken to be approximately 550 nanometers for calculations involving bias retardation. With de Sénarmont compensators, bias retardation values ranging between one-twentieth and a full wavelength can be easily measured with an accuracy of 0.15 nanometers.

Bias Retardation in de Sénarmont DIC Microscopy

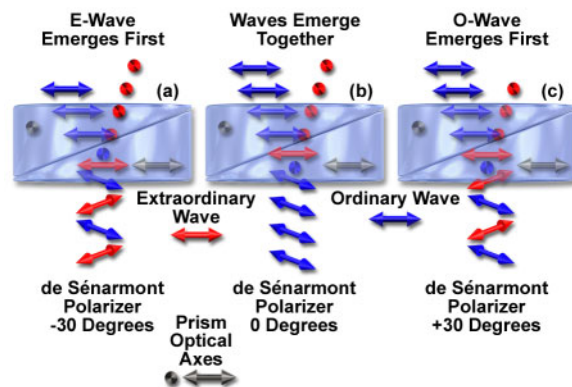


Figure 4. Origin of bias retardation in de Sénarmont DIC microscopy. Orthogonal wavefronts in phase enter the Nomarski prism, are sheared at the interference plane, and exit together. When the polarizer is rotated either to the left or right, one of the wavefronts precedes the other, thus introducing a phase difference.

The effects of bias retardation introduced into the DIC optical system by a de Sénarmont compensator are illustrated in Figure 4 for three settings of the compensator. All of the examples presented in Figure 4 diagram a single wavefront entering the central portion of a Wollaston prism, but a Nomarski prism will operate in the same fashion. When the polarizer transmission axis is aligned parallel to the fast axis of the quarter-wavelength retardation plate (Figure 3(b) and 4(b)), linearly polarized light emerges from the compensator and is incident on the lower wedge surface of the condenser Wollaston prism (as depicted in Figure 4(b)). In a DIC microscope, the incident linearly polarized light is oriented at a 45-degree angle to the fast and slow axes of the lower wedge component of the Wollaston (or Nomarski) prism. Upon entering the prism, the polarized light is separated into orthogonal components, which traverse the fast and slow axes of the lower quartz wedge and become sheared at the boundary between the two prism wedges. Because the linear wavefront exists as a single phase when it enters the prism, the orthogonal components are initially in phase when

they are produced at the air-quartz boundary, but undergo phase shifts inside the prism.

As previously described, the gain in phase by the ordinary wavefront in the lower portion of the Wollaston prism is offset in the upper wedge after the ordinary and extraordinary waves exchange identities at the junction between the two wedges. The net result is a cancellation of phase shifts produced inside the prism, and the orthogonal wavefronts emerge from the Wollaston prism in phase with each other (Figure 4(b)). In this condition, the optical system exhibits **maximum extinction**, and only large phase gradients present in the specimen are visible. These phase gradients are superimposed on a very dark, or black, background and take on the appearance of a darkfield image.

The situation is quite different when the polarizer is rotated in either direction away from the zero position in a de Sénarmont compensator. Wavefronts emerging from the compensator exhibit phase shifts that impart an elliptical or circular character to the vector summation of the orthogonal wave components. When the polarizer is rotated to the left by 30 degrees (negative bias retardation; Figure 4(a)), the ordinary wavefront generated by the de Sénarmont compensator enters the Wollaston prism prior to the extraordinary wavefront, and exits the prism (after exchanging identities) as the extraordinary wavefront ahead of the ordinary wavefront. The basic result is the generation of an optical path difference, which is required for the introduction of bias retardation. The opposite effect occurs (Figure 4(c)) when the de Sénarmont polarizer is rotated to the right (positive bias retardation), and the ordinary wavefront emerges from the Wollaston prism ahead of the extraordinary wavefront.

Regardless of whether bias is introduced into a differential interference contrast system by translating the objective Nomarski prism or by rotating the polarizer on a de Sénarmont compensator, the net result is the same. In a properly configured microscope that is correctly aligned for Köhler illumination, an image of the light source and condenser prism is transferred by the optical system (condenser and objective) onto the inverted second Nomarski prism located at the objective rear focal plane. The linear phase shift across the face of the condenser prism is precisely compensated by an opposite phase shift in the objective prism. **Translation of the objective prism along the shear axis does not alter the phase shift distribution, but instead, adds or subtracts a constant phase difference across the entire microscope aperture.** In the same manner, rotating the polarizer in a de Sénarmont compensator also introduces a variable and controlled phase difference. The matched prism system enables image formation to occur with the same bias retardation for every wavefront pair projected from the condenser aperture, irrespective of the route through which it traverses the specimen to reach the objective.

Presented in Figure 5 is a series of digital images recorded in differential interference contrast using a bias retardation range of one-twentieth to a quarter wavelength in several intermediate steps. The specimen is a 5-micrometer (thickness) preparation of human buccal mu-

cosa epithelial (cheek) cells spread on a microscope slide in buffered saline solution and imaged through a 170-micrometer cover glass. The cells exhibit regions of fluctuating thickness, which range from approximately 1 to 4 micrometers. Rendition of specimen detail and the shadow-cast pseudo three-dimensional effects are the most pronounced at the lower bias retardation values (Figure 5(a)), but contrast and definition of fine specimen detail both deteriorate as bias retardation is increased (Figure 5(b) through 5(d)). At the highest bias retardation value (one-quarter wavelength; Figure 5(d)), contrast is extremely poor and very few structural details are visible. For this particular specimen, the optimum retardation range appears to lie between one-twentieth and one-twelfth of a wavelength.

As the optical path gradient in a specimen increases in DIC microscopy, so does image contrast. Altering the bias retardation to varying degrees can also produce significant contrast fluctuations in the specimen as observed in the eyepieces (Figure 5). In general, the optimum degree of displacement between the ordinary and extraordinary wavefronts induced by translation of the objective prism, or by rotating the polarizer in a de Sénarmont compensator, is on the order of less than one-tenth wavelength. However, this value is largely dependent on specimen thickness, and the useful range of bias retardation for biological specimens lies between one-thirtieth and a quarter wavelength. Contrast in specimens having very large optical gradients can often benefit from even greater bias retardation values (up to a full wavelength). The introduction of bias retardation into a differential interference contrast microscope enables phase specimens to be observed with greater ease, and dramatically facilitates imaging efforts with traditional film or digital camera systems.

Bias Retardation with de Sénarmont Compensation

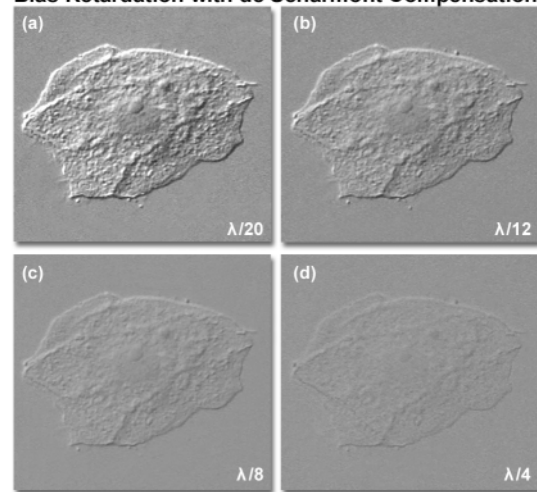


Figure 5. Human buccal mucosa epithelial (cheek) cell imaged in de Sénarmont DIC with varying levels of bias retardation indicated on the image panels.

Compensator Retardation Plates in de Sénarmont DIC Microscopy

Commonly referred to as **compensating** or **retardation** plates in the field of polarized light microscopy, compensators can be utilized in DIC microscopy to manipulate the amount of contrast obtained from bias retardation between the ordinary and extraordinary wavefronts. Compensating plates bestow greater control for adjusting the contrast of specimen details in relation to the background intensity and color values, and also enable more precise tuning of the bias retardation between wavefronts. These birefringent components are also frequently employed for **optical staining** of transparent specimens, which are normally rendered over a limited range of grayscale values (1).

On microscopes equipped with a de Sénarmont compensator for introducing bias into a differential interference contrast optical system, a full-wave retardation plate can be added to optically stain the specimen with Newtonian interference colors and provide more quantitative information about path differences (illustrated in Figure 6). Retardation plates can be inserted into the optical pathway of a de Sénarmont DIC microscope between either the objective prism and the analyzer or the compensator and the condenser prism. Many microscopes have a slot located in the intermediate tube or substage condenser housing designed for this purpose. Addition of a first-order compensator (often termed a **full-wave** or **first-order red** retardation plate) having a retardation value equal to a full wavelength in the green region of visible light (approximately 550 nanometers), introduces a spectrum of interference colors to the specimen and background (Figure 6). With the compensator in place, green light is unable to pass through the analyzer because it emerges from the retardation plate linearly polarized with an electric field vector having the same orientation as the polarizer. However, wavefronts in the red and blue spectral regions experience retardations less than a wavelength and become elliptically polarized, enabling them to pass a component through the analyzer. As a result, these colors become mixed to form a magenta background in the field of view.

When a specimen is observed in white light (tungsten-halogen illumination) with a de Sénarmont DIC optical system and a first-order retardation plate, the background appears magenta while image contrast is displayed in the second-order blue and first-order yellow colors (depending upon orientation) of the Newtonian interference color spectrum. With the retardation plate inserted into the light pathway, small variations in bias retardation obtained by rotating the polarizer in a de Sénarmont compensator yield rapid changes to interference colors observed in structures having large optical path length gradients. This technique is useful for introducing color (optical staining) to regions having high refractive index boundaries, such as cellular membranes, large intracellular particles, cilia, and the nucleus. The interference colors displayed by specimen features can be compared to the values on a Michel-Levy color chart in order to obtain an estimate of the optical path difference.

Illustrated in Figure 6 is a typical semi-transparent specimen that has been imaged through both standard bias retardation techniques and optical staining, and rendered in pseudo three-dimensional relief with a vivid display of color. Figures 6(a) and 6(b) depict an *Obelia* hydroid polyp, which displays a significant amount of structure at low to intermediate bias retardation values (Figure 6(a)), but also exhibits an abundant spectrum of color with a retardation plate in the light path (Figure 6(b)). Optical staining can also be useful to produce color reversal of shadow-cast effects. Although the images presented in Figure 6 do not reveal hidden scientific information pertaining to the specimens, they do have the potential to advance the technique of DIC optical microscopy as a legitimate bridge between science and art.

Interpretation of de Sénarmont DIC Images

By observing the shadow-cast orientation present in almost every image produced through bias retardation introduced by a de Sénarmont compensator, the direction of optical shear is obvious and can be precisely defined as the axis connecting regions displaying the highest and lowest intensity (amplitude) values. The level of contrast bestowed on specimen phase gradients (and the degree of pseudo three-dimensionality) by de Sénarmont DIC is a function of the amount of bias retardation introduced into the optical system by rotating the polarizer in the compensator (1-4). Because the shear axis is fixed by Nomarski prism design, and other constraints involved in wavefront orientation for DIC microscopy, the axis direction cannot be altered to affect specimen contrast through a simple setting on the microscope. However, the relative phase retardation between ordinary and extraordinary wavefronts can be reversed by rotating the de Sénarmont compensator polarizer to the corresponding negative value. When the phase retardation is altered as just described, the orientation of bright and dark edges on the specimen is reversed by 180 degrees. In essence, the only mechanism available to the microscopist to change the shear axis relative to the specimen is to reorient the specimen itself, a maneuver that benefits from the utilization of circular 360-degree rotatable stages.

Each specimen examined in de Sénarmont DIC microscopy will have an optimum bias retardation setting of the compensator that generates a maximum level of contrast in the final image. Very thin specimens that display a shallow refractive index gradient, such as living cells in culture, generally benefit from equally low bias settings (small translations of the polarizer) only slightly larger than the largest phase shift present in the specimen (on the order of approximately one-twentieth of a wavelength, or about 30 nanometers). However, thicker specimens often require higher bias settings (up to a quarter-wavelength) at large condenser apertures to produce satisfactory results, usually through optical sectioning. Because many specimens are composed of features displaying a variety of different sizes and refractive indices, the optimum bias retard setting of the de Sénarmont compensator is usually a compromise.

Optical Sectioning with de Sénarmont DIC Microscopy

The ability to image a specimen in de Sénarmont DIC microscopy with large condenser and objective numerical apertures enables the creation of optical sections from a focused image plane that are remarkably shallow. Without the disturbance of halos and distracting intensity fluctuations from bright regions in lateral planes removed the focal point, the technique yields sharp images that are neatly sliced from a complex three-dimensional phase specimen. This property is often utilized to obtain crisp optical sections of cellular outlines in complex tissues with minimal interference from structures above and below the focal plane.

In all traditional forms of transmitted and reflected optical microscopy, the condenser aperture iris diaphragm plays a major role in defining image contrast and resolution. Reducing the aperture size increases the depth of field and overall image sharpness while simultaneously producing enhanced contrast. However, if the condenser diaphragm is closed too far, diffraction artifacts become apparent and resolution is sacrificed. Often, the optimum aperture diaphragm setting is a compromise between accurately rendering specimen detail in sufficient contrast and retaining the resolution necessary to image minute features while avoiding diffraction artifacts.

When the condenser iris diaphragm is adjusted to approximately 70 percent of the objective rear aperture size, most high-performance de Sénarmont DIC optical systems produce excellent contrast. However, these microscopes also perform superbly when the condenser diaphragm is opened to match the objective rear aperture diameter. In order to achieve the optimum balance between resolution and contrast for optical sectioning experiments, it is critical that the microscope be properly configured for Köhler illumination and the Nomarski prism components, analyzer, and de Sénarmont compensator be accurately aligned.

Optical sections taken of a living *Volvox* colony using de Sénarmont DIC to achieve bias retardation on an inverted tissue culture microscope are illustrated in Figures 6(c) and 6(d). The aquatic microorganism is composed of hundreds to thousands of identical green algae cells having approximately the same diameter, but organized into several morphological motifs. On the periphery of the colony, individual cells are arranged in a semi-transparent widely spaced layer termed the **mucilage**, as illustrated in Figure 6(c). Farther into the mass, the colony forms several concentrated spherical groups of reproductive cells, termed **gonidia**, which produce small daughter colonies within the parent colony (Figure 6(d)). As the microscope is focused on the uppermost layer of the colonies in the mucilage (not illustrated), structural detail in the individual cells becomes visible, but many cells are masked by the daughter colony.

Thin biological specimens (10 to 20 micrometers in thickness) usually produce poor optical sections at lower magnifications, but often reveal substantial internal detail when visualized with high magnification objectives

Optical Staining and Sectioning with de Sénarmont DIC

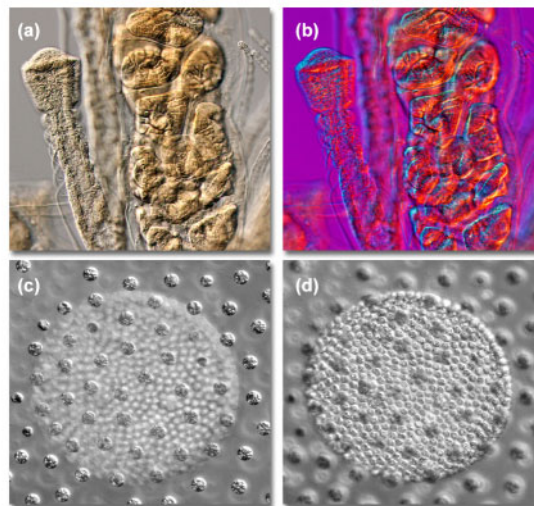


Figure 6. Optical staining and optical sectioning with de Sénarmont DIC microscopy. (a) and (b) *Obelia* colony imaged without (a) and with (b) a full-wave retardation plate. Optical sectioning (c) and (d) of a *Volvox* colony.

having large numerical aperture (60x and 100x). Thicker specimens can be readily sectioned at low magnifications where aberration is minimized. Collection of optical sections from thicker biological specimens, especially those immersed in aqueous saline or buffered solutions, is often hampered by spherical aberration produced by refractive index discontinuities at the interface between the cover glass and mounting medium. This artifact will reduce resolution at higher penetration depths in the optical section series.

Conclusions

In differential interference contrast microscopy, a phase difference is introduced by geometric path length and refractive index variations of the specimen into the two orthogonal wavefronts generated by the Nomarski prism housed in the condenser. The net result is elliptical polarization between the wavefronts that are recombined by the objective Nomarski prism and subsequent image formation as a component of these waves passes through the analyzer. Bias retardation can be introduced to the system by translating the objective prism along the microscope optical axis or by combining a quarter-wave-length plate with the polarizer or analyzer (de Sénarmont compensation). Thus, optimum contrast, field brightness, and sensitivity can be gained by simple rotation of a control knob. There are several advantages to using de Sénarmont compensation DIC microscopy instead of the traditional configurations that rely on translation of the objective Nomarski prism, and these benefits are partially responsible for the increasing popularity of the technique.

A quantitative determination of the exact amount of bias retardation applied to the optical system is difficult

to ascertain with a majority of DIC microscopes that employ a translating Nomarski prism in the objective rear focal plane. In some cases, Nomarski prism frames with highly accurate micrometer-controlled translation devices have been developed, and these components can be utilized to accurately gauge the amount of bias introduced by moving the prism in small increments. However, any DIC microscope can be configured for accurate bias retardation measurements using de Sénarmont compensation simply by adding a graduated rotating polarizer or analyzer and a fixed quarter-wavelength retardation plate to the optical train.

Another important advantage of de Sénarmont DIC compensation is the proximity of these components to important image forming and aperture conjugate planes in the microscope optical train. Microscopes designed with sliding objective Nomarski prisms must physically translate the compound prism element across the optical pathway while the microscopist observes the level of bias retardation applied to the system. In many cases, especially if the prism frame fits loosely in the mount, serious image shifts can occur during prism translation, which impede the ability to observe the specimen and to capture images. Image shifts cannot occur during introduction of bias retardation with a de Sénarmont DIC microscope, primarily because the compensator retardation plate and rotating polarizer are positioned before the condenser or after the objective, in the microscope illumination pathway, and not within the image forming optical elements. This difference should be a major factor to be considered when choosing a microscope configuration for quantitative DIC experiments.

Ergonomic considerations are also important when comparing traditional and de Sénarmont DIC microscope configurations. Modern microscopes are designed with stage and focus control knobs that are positioned on the front of the microscope base, at desktop height, and within easy reach of the operator. These features allow a more relaxed posture with the hands resting comfortably on the desktop to help eliminate fatigue and reduce the possibility of stress, which can ultimately lead to neuromuscular disorders. In a traditional DIC microscope, the operator must continuously raise a hand (and arm) to a level above the objective in order to adjust the position of the Nomarski prism. However, in ergonomic de Sénarmont designs, the compensator assembly is positioned on the microscope base over the front illumination port, very near the lowered focus knobs and stage translational control levers. The close proximity of all microscope control mechanisms on these DIC microscopes dramatically reduces operator fatigue during long periods of continuous observation.

Enhanced video microscopy techniques take advantage of accurate bias retardation values introduced by de Sénarmont compensators. Often referred to by the acronym **VE-DIC** (video-enhanced differential interference contrast), the technique is capable of recording specimen fine structural detail that is beyond the optical resolution of a compound microscope. Video-enhanced DIC microscopy has been a powerful research tool in cellular biol-

ogy for measuring the assembly dynamics of individual microtubules and visualizing the motion of bacterial flagella, both of which are not resolved using other techniques. As discussed above, a majority of very thin DIC specimens are best observed at bias retardation values averaging one-twentieth of a wavelength. However, when video-enhanced DIC is employed to image sub-resolution specimens (such as microtubules and miniature organelles), bias retardation values down to approximately one hundredth of a wavelength must be employed. Obviously, these very slight levels of retardation are best achieved with de Sénarmont compensators designed with highly accurate, graduated and vernier-equipped, rotating polarizer (or analyzer) assemblies.

Among the chief imaging advantages of differential interference contrast microscopy, regardless of the mechanism by which bias retardation is introduced, is that (unlike darkfield or phase contrast) the image of smaller specimen features is not obscured by adjoining regions having large optical path gradients. In addition, the shadow-cast appearance of the image on a neutral gray background, coupled to the sensitivity for imaging very small features together with those much larger (for example, minute appendages to living cells or dynamic inclusions and moving organelles within a cell), is a significant improvement over traditional contrast-enhancing techniques. These benefits, in addition to the wide dynamic range of contrast control and shallow depth of field, have all contributed to the widespread popularity of the technique.

Selected References

1. Murphy, D. B., *Fundamentals of Light Microscopy and Digital Imaging*, Wiley-Liss, New York, pages 43-59 (2001).
2. Schwartz, S., Murphy, D. B., and Davidson, M. W., *Differential Interference Contrast Microscopy*, Molecular Expressions (<http://microscopy.fsu.edu>) and MicroscopyU (<http://www.microscopyU.com>) websites (2003).
3. Pluta, M., *Advanced Light Microscopy, Vol. 2, Specialized Methods*, Elsevier, New York, pages 145-197 (1989).
4. Lanni, F. and Keller, E. in *Imaging Neurons: A Laboratory Manual*, Yuste, R., Lanni, F., and Konnerth, A. (eds), Cold Spring Harbor Laboratory Press, Cold Spring Harbor, New York, pages 1.30-1.37 (2000).
5. Pluta, M., *Phase Contrast and Differential Interference Contrast Imaging Techniques and Applications, SPIE Proceedings 1846*, International Society for Optical Engineering, pages 10-25 (1994).
6. Slayter, E. and Slayter, H., *Light and Electron Microscopy*, Cambridge University Press, Cambridge, United Kingdom, pages 154-158 (1992).